



Research Article

Centralized controller-based on optimal power flow (OPF) algorithm for power management in microgrid systems

Abumuslim KHUJAEV^{1,*} , Abbas UĞURENVER¹

¹Institute of Graduate Studies, Department of Electrical and Electronic Engineering, Istanbul Aydın University, Istanbul, 3472945, Türkiye

ARTICLE INFO

Article history

Received: 06 July 2024

Revised: 21 August 2024

Accepted: 22 October 2024

Keywords:

Centralized Controller;
Renewable Energy; Microgrid
System; Optimal Power Flow;
Power Management; Solar PV

ABSTRACT

The advent of renewable energy sources and their power management in microgrid (MG) systems have seen significant changes recently. Efficient and reliable power management is one of the key strategies in developing microgrid systems. This paper studies and analyzes the microgrid system with an optimal power flow (OPF) algorithm-based power management method. The proposed OPF will work as a centralized controller, enhance the switching between energy sources, dynamic loads, batteries and main grid to ensure efficient, reliable and sustainable power management and enhanced performance for the microgrid system. Microgrids are technologically advanced systems that are incorporated with different types of energy sources which connect and disconnect the sources with the main grid based on the system condition. In other hand, microgrids with uncontrollable energy sources and loads can have variation in power flow. The rapid changes in the system will lead to poor power quality. The system contains a solar PV, a battery energy storage system (BESS), an electric vehicle (EV), main grid and dynamic loads. optimal power flow receives inputs from microgrid system and target output to optimize stability, reliability and efficiency in power quality. Simulations were carried out based on MATLAB/Simulink and the OPF used as a centralized controller and the results obtained enhanced the power quality of microgrid systems. The system was analyzed in three different scenarios, in normal condition, abnormal condition of solar PV and abnormal condition of batteries. Hence, the proposed OPF enhanced the power quality, optimized performance of switching between energy sources and main grid.

Cite this article as: Khujaev A, Uğurenver A. Centralized controller-based on optimal power flow (OPF) algorithm for power management in microgrid systems. Sigma J Eng Nat Sci 2025;43(6):2279–2293.

INTRODUCTION

In today's rapidly growing world, the production of electricity increased significantly due to industrialization,

population growth, and high demand for electrical power for electric appliances. Electricity is generated from a range of energy sources, such as coal, natural gas, and renewable energy sources <] analyzed a multi-level inverter based

*Corresponding author.

*E-mail address: abumuslimkhujaev@stu.aydin.edu.tr

*This paper was recommended for publication in revised form by
Editor-in-Chief Ahmet Selim Dalkilic*



three-phase system during dynamic load condition. The controller is developed to supply real power even with the variation happened in voltage and current. The proposed method promised enhanced performance at DC voltage level. Moreover, theoretical model was evaluated with real time data. A DC-DC boost buck converter is a crucial component of the power system which has a MOSFET switch, traditional buck converter, capacitors and inductors. Author in [30] proposed a technique that is more reliable than the conventional converter. The proposed method had better result in terms of switching frequency and dynamic load. Another article used bidirectional buck-boost converter to improve dc voltage for the grid system [31]. This is done by minimizing the inductor current and inductor current ripple. The experimental results showed better results than the conventional type of buck boost converter. Hence, the controller was not used in an AC/DC microgrid system.

Author in [32] presented an optimal power flow (OPF) controller used in hybrid microgrids. The author claimed that the plugging and un-plugging of appliances can penetrate the flow of power in the system. Especially during islanded mode, the appliances require fast response to overcome the variation in voltage and current of the loads. Therefore, the MG system require steady state stability by employing OPF to operate efficiently. The proposed technique is used in an AC/DC system to maximize its control strategy and overcome economic challenges in the future. Another author has examined the issues and challenges encountered by power systems over the past decade [33]. The author used grey wolf optimization technique to have robust control over microgrid system. The system included diesel, engine solar PV, and battery systems. The proposed method offers an improved dispatching technique for loads and sources, ensuring an economical power supply while minimizing reliance on the main grid. MATLAB/Simulink is used to validate results. However, the author did not study the OPF algorithm in real time to see if it can improve the performance of the microgrid system. A non-linear controller for renewable energy sources were studied in a DC microgrid systems. Author claimed that the conventional PI controller used in MG systems was short in providing robust control and stable power distribution in the system [34]. Moreover, interconnection damping assessment-passivity based controller (IDA-PBC) is employed to regulate the DC-link of the system. The proposed controller was tested in three different conditions and experimental results were presented. Hence, the controller was not used in AC/DC microgrids.

Summary

The following Table 1 presents the comparison of different controllers used in microgrid system.

For the basis of the following paper, the optimal power flow algorithm-based power management strategy, performance of an AC/DC hybrid microgrid, renewable energy source, and energy storage system were studied. The study

was conducted accordingly, and I present my acknowledgement to authors who contributed to developing hybrid microgrid systems. Referring to the above studies there were several controlling techniques to enhance power flow and managing microgrid systems. Many articles used controllers and converters to improve performance of the power system. Moreover, switching techniques between grid-connected and islanded modes were seen in some of the studies. An article studied the AC/DC microgrid system powered by DC power sources [37]. However, the author did not implement real-time values to show correctness of the controller in real-time scenarios. Overall, the summary of the research focused on developing controllers to maintain optimal power flow in microgrid systems. However, several challenges in AC/DC microgrid systems remain unaddressed by the authors cited in the literature review. The AC/DC hybrid microgrid system requires renewable energy sources and backup batteries to support the grid during periods of low solar PV irradiance. It also needs the capability to switch between grid-connected and islanded modes and a centralized controller to always manage the switching. The issues must be addressed, and proper component selection is essential. An optimal power flow algorithm-based power management is required to achieve enhanced power flow in microgrids. In this paper the research is going to achieve the following items. This paper aims to achieve the following objectives.

1. Creating an AC/DC microgrid system.
2. Identifying sources and loads for the system.
3. Identifying values for the loads and sources.
4. Connecting a three-phase circuit breaker between main grid and microgrid system.
5. Analyzing the performance of the system with existing components.
6. Integrating Three-phase stand-alone inverter control design with PI controller to generate PWM signal for the switch.
7. Integrating bidirectional converters in DC sources to boost voltage regulation to a desired voltage level.
8. Integrating a centralized controller to control and provide optimal power flow to the hybrid microgrid system.
9. Analyze the effect of OPF centralized controller in three conditions such as normal condition, solar irradiance abnormal condition and batteries abnormal condition.

Microgrid System

Microgrids normally consist of loads, solar PV, battery energy storage system, electric vehicle, main grid, and they are designed to work in grid connected and islanded modes [38]. The solar PV incorporates DC-DC boost converter to boost the voltage level to a desired voltage level [39]. One of the main characteristic of MG is that they can support the MG by balancing the loads with renewable energy sources, they will be connected to the grid when the sources are not able to deliver enough power. Furthermore, when the MG is connected to the main grid it is called grid connected

Table 1. Comparison of different controllers

Ref	Controller	Disturbance	Electrical Network	Remark
[24]	GA/AC OPF Algorithm	Operational challenges of the microgrids	AC/DC microgrid	Capable of catching variation to provide enhanced power flow
[26]	Hybrid power-sharing control	Low-frequency power oscillations and dynamic load behavior	DC microgrid	Damping low-frequency oscillation
[28]	UCS	Switching challenges in islanded mode	Distributed generation (DG) network	Improved performance in grid-connected/islanded modes with no need for switching
[21]	Buck-boost converter	Voltage balancing and losses	6S1P battery pack	Showed high balancing efficiency
[35]	MPPT incorporates with a TLBC	Output voltage distortion, inductor current ripple and switching losses	PV system	Optimal power extraction from solar PV system
[31]	Bidirectional buck-boost converter	Inductor current ripple	B3CFIDC	Robust control over dc-dc voltage and current distribution
[34]	A non-linear control structure	Power losses	DC microgrid	Super-capacitor voltage regulation
[30]	DC-DC buck-boost converter	Uncertainties in microgrid systems	DC system	Better conversion ability compared to conventional controllers
[23]	Multi-stage PD(1+PI) controller	Voltage and load variation	Buck converter system	Showed better result than other buck converters
[29]	MLI	Unstable real power across the DC-link components	AC/DC microgrid system	Higher efficiency than the other types of controllers
[18]	VSC	Voltage variation during islanded mode	AC/DC microgrid system	The controller was able to provide desired voltage level even when the sources have changes
[32]	OPF	variation in load/source values when the system changes from one mode to another mode	38-bus AC/DC hybrid microgrids	more effective in hybridizing AC distribution systems
[20]	SLC	Fluctuation during dynamic load behavior	AC/DC hybrid microgrids	Maximizes efficiency for a solar PV and BESS
[19]	FCS-MPC	Uncertainties due to the loads and sources	AC/DC microgrid	Better voltage regulation in grid-connected and islanded modes
[36]	SUDC	Synchronization issues in power distribution	SUDC	The controller is capable of voltage regulation in bot grid-connected and islanded mode
[27]	DWT	IGBT switch breakdown failure	Equivalent boost converter circuit with MPPT	Enhanced performance in Microgrid system

mode, but when it is disconnected from the main grid it is called islanded mode and it connect/disconnect with a switch [40]. The reason to keep MG disconnected from the main grid is because of the disturbances, fault, and poor power quality and voltage/current fluctuation in the main grid. In islanded mode the MG enables enhanced power quality, reduces power losses, and improved system efficiency [41]. There are AC, DC and hybrid MG (AC/DC) MG systems. Depending on the requirements of the sources used, and types of loads one need to choose what type of MG is suitable for their design. For only DC components a DC MG is suitable to include, for AC loads and AC sources one should use AC MG system. However, when having the mixture of DC and AC energy sources and loads one should

use hybrid MG system [42]. A hybrid MG contains one DC bus and one AC bus, and all the AC/DC sources and loads are connected through AC/DC buses depending on their configuration. The benefits of using hybrid MG is that it minimizes the use of too many converters and buses and it ensures cost effective design [43].

A MG normally incorporates energy sources, loads and energy storage systems. For a typical MG systems energy sources are located close to the residents. Solar PV, BESS, EV are examples of the distributed energy resources (DER) s [44, 45]. Therefore, DER located close to the users will help the system to lower the amount of power losses. The power generation by only solar PV system is unpredictable. Therefore, it is essential to include ESS systems to ensure

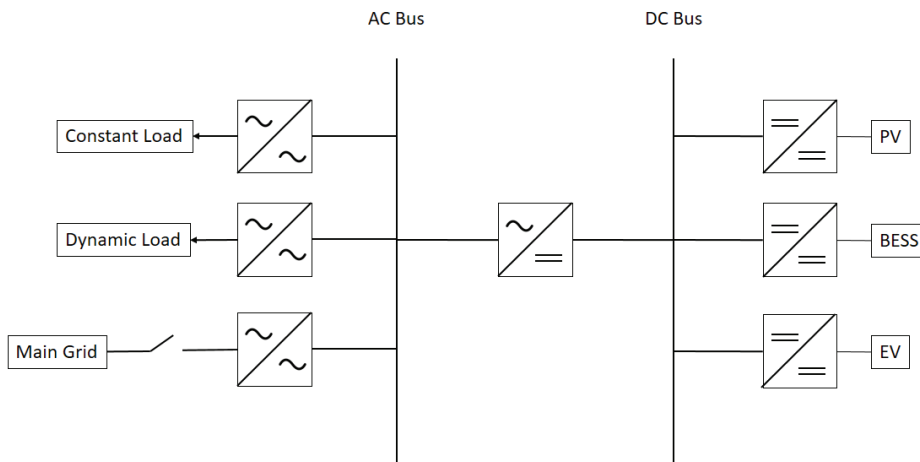


Figure 1. The hybrid microgrid model.

Table 2. The nominal values for the AC and DC buses, frequency and nominal voltage for the MG

Item	Nominal value
$freq_n$	50 Hz
AC V_n	400 V
DC V_n	400 V
R_{grid}	1.8
L_{grid}	4 μH

reliability in the MG [46]. In case of high-power generation by the solar PV the ESS systems allows charging and discharge when the power generation is low or the electricity tariffs are high. There are many types of ESS to store energy and one of the common used batteries are lithium-ion batteries. The MG includes a dynamic load and a constant load. Figure 1 shows the type of MG system used in this paper. The actual design of the MG system is shown in Appendix 1.

The MG model was built and tested in MATLAB/Simulink and some nominal values presented in Table 2.

The solar PV is used as an energy source that supply power to MG. The solar PV array delivers maximum power point of 218.871 W. The power generation by a solar panel is highly dependent on solar irradiance (SI), the normal level for a solar PV is 1000 W/m². In this paper the temperature is neglected. The formula for solar PV is given in equation 1. To increase the total power generated from solar PV, it is necessary to expand the number of solar panels to the desired amount, as illustrated in equation 2 [47, 48].

$$P_{module} = \frac{\text{Solar Irradiance } (\frac{W}{m^2})}{1000 (W)} \times \text{Maximum Power (W)} \quad (1)$$

$$\text{Total } P_{pv} = \text{Parallel strings} \times \text{Series} \\ - \text{connected modules per string} \times P_{module} \quad (2)$$

The nominal value for solar PV is shown in Table 3.

Table 3. Specifications of solar PV panel

Item	Value
P_{module}	218.871
Parallel strings	6
Series-connected modules per string	15

The battery storage system includes a lithium-ion battery and the specifications for the battery are given in Table 4.

Table 4. Specifications of BESS battery

Item	Value
Nominal voltage (V)	120
Rated Capacity (Ah)	180
Initial state-of-charge (%)	50
Battery response time (s)	0.1

The EV source includes a lithium-ion battery and the specifications are given in Table 5.

Table 5. Specifications of EV source

Item	Value
Nominal voltage (V)	120
Rated Capacity (Ah)	180
Initial state-of-charge (%)	50
Battery response time (s)	0.1

The constant load and dynamic load values are mentioned in Table 6. The dynamic loads fluctuated based on the demand changes throughout the day.

Table 6. Specifications of the constant load and dynamic load.

Item	Value
Constant load (W)	8000
Dynamic load (W)	5000~10000

Optimal Power Flow

The MG power management works based on OPF model and the OPF works as a centralized controller to enhance the efficiency and reliability of the MG system. The centralized controller receives information from MG, process it and gives reference current to EV and connect/disconnects the switch in MG system. The OPF model is used to reduce excess power losses and costs for the system. There many types of OPF can be used to calculate the output and process it in the MG. However, to measure the values throughout the day, dynamic load changes, dynamic solar irradiance and other components makes the analysis quiet challenging. Therefore, this paper analyzes the MG system in MATLAB/Simulink with linear programming codes to enhance the performance of the system. The inputs and the outputs for the centralized controller based on OPF is shown in Figure 2. The simulation run for 2.4 seconds as the system takes long time to run if the simulation time increases. 2.4 seconds considered as 24 hour or a day.

Flow chart chart of the optimal power flow algorithm

The paper's OPF is built to minimize the power losses and always keep THE MG at its maximal stable condition. Initially the working condition of MG is examined and then the predictions and OPF values are studied. The OPF and prediction values from time t were sampled then prediction values t+Δt , were predicted. The values that were sampled

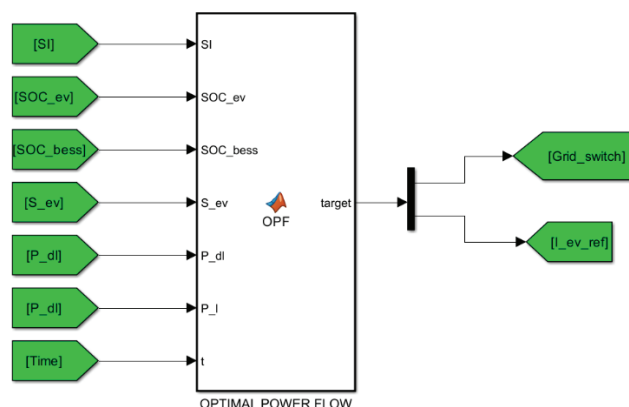


Figure 2. Centralized controller based on OPF algorithm.

were solar irradiance PV, loads, BESS and state of charge of electric vehicle. The optimized value for the output includes grid switch and reference current for the EV. The flow chart of the centralized controller for microgrid power management is presented in Figure 3.

Microgrid components and their function

The following Table 7 shows how the system works to process in OPF algorithm and maintain its efficient performance.

The OPF function in isnladed mode

The aim of the OPF is to minimize the power difference between the power generated and load demand. The total power generated from energy sources were summed and the loads were summed at every hours. The total load power then was subtracted from total source power to show the minimum result to keep the Microgrid in islaned mode. In islaned mode, the net power indicates that the generated power is greater than the load demand. The formulas are presented in equation 3, equation 4, and equation 5. The BESS power, and EV power are dependent on SOC charge percentage. If state of charge is zero both the batteries cannot deliver any power to the microgrid system.

$$P_G = P_{pv} + (P_{bess} \times SOC_{bess}) + (P_{ev} \times SOC_{ev}) \quad (3)$$

$$P_L = P_{dl} + P_{cl} + P_{losses} \quad (4)$$

$$P_{net} = P_G - P_L \quad (5)$$

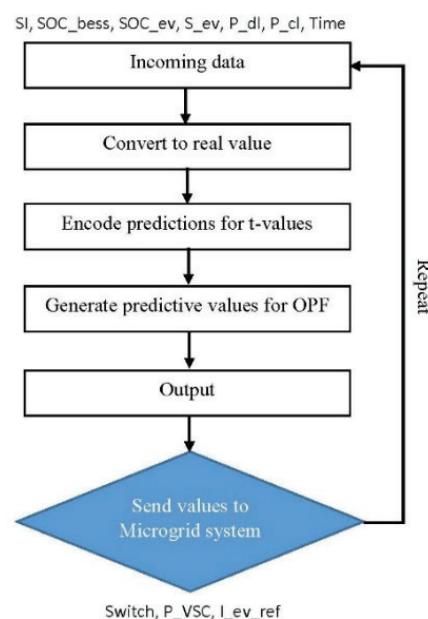


Figure 3. The flow chart of the centralized controller for microgrid power management.

Table 7. Shows the working principles of the MG components

Grid Switch	It is only closed and ensures the MG to supply itself from PV, BESS and EV sources as much as it can. It is only closed when the power generated by the PV, BESS and EV cannot supply enough power is lower than the loads power in the MG. Therefore, the disturbances are neglected in the OPF.
Solar PV	The solar PV generates power based on solar irradiance throughout the day. It does not supply power to the MG when the switch is in grid connected mode. Moreover, the temperature is not considered in this paper.
BESS	The BESS can charge from PV panel and it does not supply any power when the MG is in grid connected mode.
EV	The EV battery connect/disconnect from the MG. In grid connected mode it does not supply any power to the MG.
Constant Load	It is constant.
Dynamic Load	The dynamic load fluctuates during the day.

Table 8. State of charge for BESS and EV batteries

Item	Value
$SOC_{BESS} \text{ (min)}$	1%
$SOC_{BESS} \text{ (max)}$	99%
$SOC_{EV} \text{ (min)}$	1%
$SOC_{EV} \text{ (max)}$	99%

The limitations for the state of charge for BESS battery, EV battery, and maximum power for BESS battery, and EV battery are presented in equation 6-9. The system must not cross this limits. The maximum power for both the BESS battery, and EV batteries are 9kW. The maximum state of charge of BESS battery and the minimum state of charge for BESS battery is presented in Table 15. The maximum state of charge of EV battery and the minimum state of charge for EV battery is also presented in Table 8.

$$SOC_{BESS} \text{ (min)} \leq SOC_{BESS} \leq SOC_{BESS} \text{ (max)} \quad (6)$$

$$SOC_{EV} \text{ (min)} \leq SOC_{EV} \leq SOC_{EV} \text{ (max)} \quad (7)$$

$$-P_{BESS} \text{ (min)} \leq P_{BESS} \leq P_{BESS} \text{ (max)} \quad (8)$$

$$-P_{EV} \text{ (min)} \leq P_{EV} \leq P_{EV} \text{ (max)} \quad (9)$$

The output control values are presented as in formula 10.

$$Target \text{ (Output)} = Switch, P_{VSC}, I_{EV_REF} \quad (10)$$

The OPF function in grid connected mode

In grid connected mode, the microgrid does not take power from DC bus sources. As in islanded mode, the measurements will be differentiated, and the results will dictate which parameters need to be controlled in the output. The system is grid-connected when the generated power from the DC bus is less than the load demand.

The formulas are presented in equation 11, equation 12, and equation 13. Moreover, when the system is grid connected, the BESS battery charge itself from solar PV panel

power generation. The EV battery do not discharge when it is disconnected from the system nor it charges. It only works by receiving reference current from the OPF controller.

$$P_G = P_{pv} \quad (11)$$

$$P_L = P_{dl} + P_{cl} + P_{losses} \quad (12)$$

$$P_{net} = P_G - P_L \quad (13)$$

The system limitations are presented in equation 14-17. The system must not cross this limits to remain at grid connected mode.

$$SOC_{BESS} \text{ (min)} \leq SOC_{BESS} \leq SOC_{BESS} \text{ (max)} \quad (14)$$

$$SOC_{EV} \text{ (min)} \leq SOC_{EV} \leq SOC_{EV} \text{ (max)} \quad (15)$$

$$-P_{BESS} \text{ (min)} \leq P_{BESS} \leq P_{BESS} \text{ (max)} \quad (16)$$

$$-P_{EV} \text{ (min)} \leq P_{EV} \leq P_{EV} \text{ (max)} \quad (17)$$

Predictions of time varying components

Microgrid system is simulated based on time varying data. Thus, it is necessary to make predictions to make the system to work more effectively, provide the most accurate result for the outputs of the OPF controller. The dynamic values of the system are state of charge for BESS and EV batteries, solar irradiance, dynamic load and EV switch. The values received from these components need to give prediction for better performance and to be stimulated in timely basis.

The predicted results then will be processed to give output for the grid switch, reference power for the voltage source converter, and reference current for the EV battery. The input $i(t)$ values are presented in equation 18.

$$i(t) = [SI(t) \ SOC_{BESS}(t) \ SOC_{EV}(t) \ P_{dl}(t) \ S_{EV}(t)] \quad (18)$$

The predicted values are presented in equation 19.

$$i(t + \Delta t) = [SI(t + \Delta t) \ SOC_{BESS}(t + \Delta t) \ SOC_{EV}(t + \Delta t) \ P_{dl}(t + \Delta t) \ S_{EV}(t + \Delta t)] \quad (19)$$

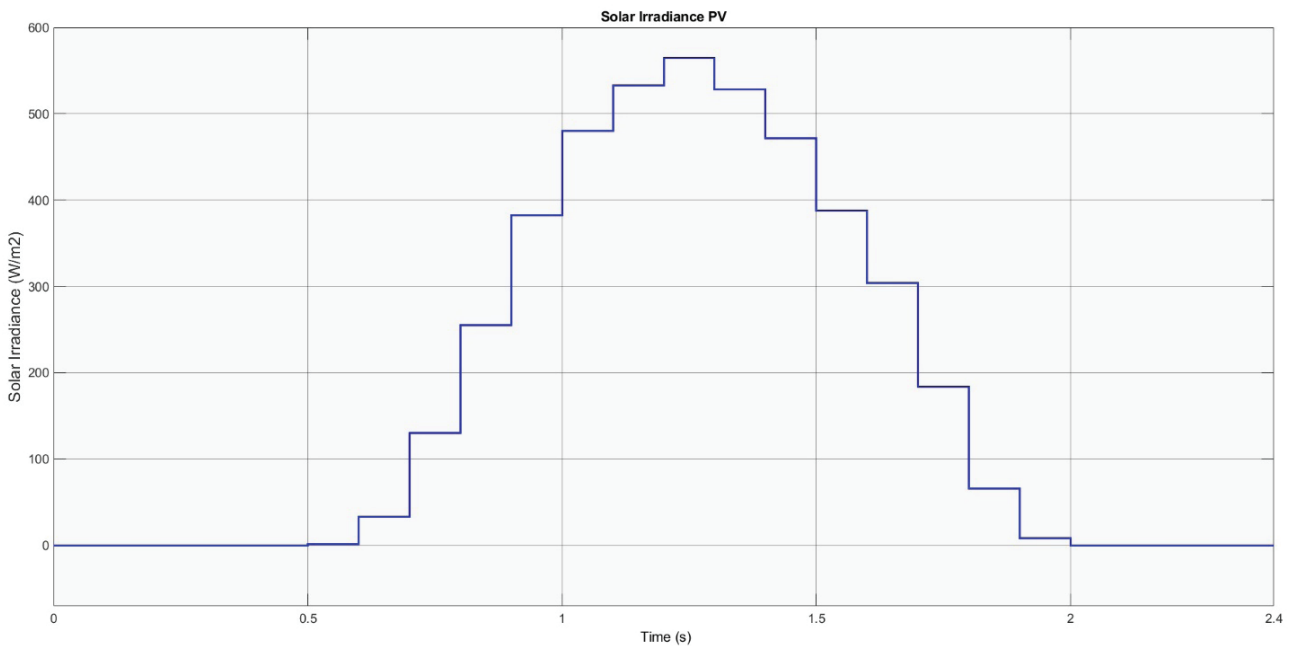


Figure 4. Shows the solar irradiance of the PV panel throughout the day.

Each predicted values are processed based on their characteristics and power performances.

The BESS battery discharges when the switch is islanded and charges from the solar PV during the grid connected mode. The EV system also performs as BESS battery, but the EV is assumed to be disconnected from 8 morning to 16 evening and from 18 evening to 20 evening.

The grid switch is either to be connected or disconnected is determined by the net power in the MG. If the generated power exceeds the load power, the MG can sustain itself, but it will supply power from main grid if the generated power is less than load power. The formula is shown in equation 20.

$$P_{net} = P_{gen} - P_l \quad (20)$$

Initially, it is verified whether the PV can supply energy to the loads. If the power from the PV is insufficient, the batteries must discharge to meet the load demand. When in grid-connected mode, the batteries are charged by the solar PV. The net power determines if the system operates in islanded mode (OPF) or grid-connected mode. In grid-connected mode, changes in the grid switch and reference current EV can be observed.

RESULTS AND DISCUSSION

The simulations and analysis of the MG system and OPF as a centralized controller were conducted in MATLAB/Simulink and the results were presented in this section of the paper. The outputs from the OPF are the reference values for grid switch, power to the voltage source converter

and reference current for EV system and they were analyzed in all conditions. Later, the results of grid power, total solar PV power, BESS power, EV power and the loads power were presented in this paper. Finally, the voltage at the DC bus, voltage of the grid system and the current from the voltage source converter were presented.

The results were obtained based on three conditions as mentioned below.

- Normal Condition
- Abnormal solar irradiance PV, where the sun disappears, and the irradiance drops to zero.
- A condition where both battery energy storage system and electric vehicle experience zero charge.

The results in each condition then were discussed at the end of this section.

Normal condition

The simulation results show the performance of the OPF as a centralized controller in normal condition. The grid switch goes to grid connected mode twice throughout the day, the power to the voltage source converter follows the switching mode and the reference current changes a lot during the day as shown in Figure 5. The grid is islanded at (switch=1) and grid-connected at (switch=0).

The results for the power of the MG units are presented in Figure 6. The grid power activates twice when the MG is grid-connected, the PV power increases when the solar irradiance increases. The power results of dynamic load, constant load, BESS battery and EV batteries are also presented during normal condition.

The results for voltage of the grid system, the current from the voltage source converter, and the voltage at the

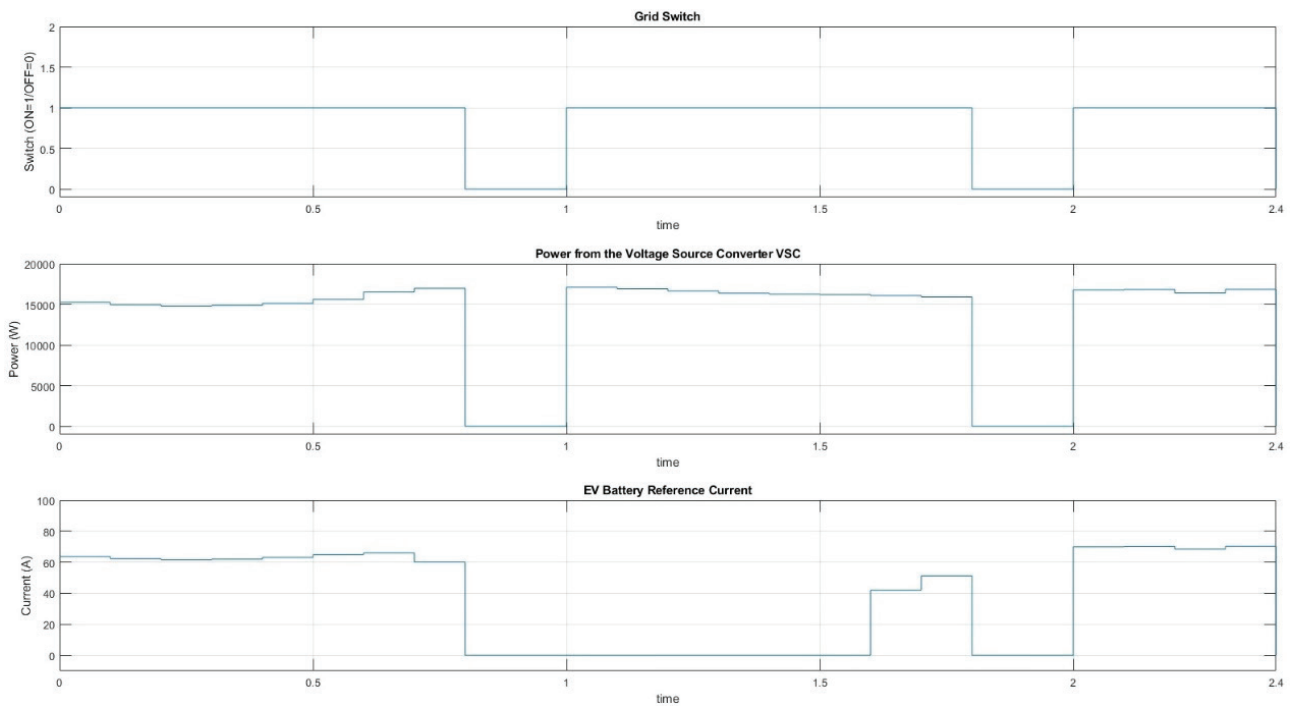


Figure 5. Shows the grid switch, power from the VSC, and the EV battery reference current in normal condition.

DC bus are presented in Figure 7. After changes occur in switching modes the voltages experience voltage surge and it stabilizes shortly. The fluctuations occurred at 0.8s, 1s, 18s and at 2s. The DC bus and voltage at the grid side were able to maintain 400 V at all time.

Solar irradiance abnormal condition

Here, the results are presented in solar irradiance PV abnormal condition, where the sun follows irradiance output until 1.2 seconds and then goes to zero. In this case, MG system will experience changes in switching. The sudden

change in solar irradiance changes the performance of the grid switching mode. Here, the grid switch experience islanded mode three times and followed by the power from the VSC. The EV battery reference current changes many times throughout the day. The grid is islanded at (switch=1) and grid-connected at (switch=0). The results are presented in Figure 8.

The power results of the grid, solar PV, dynamic load, constant load, BESS battery and the EV battery are presented in Figure 9.

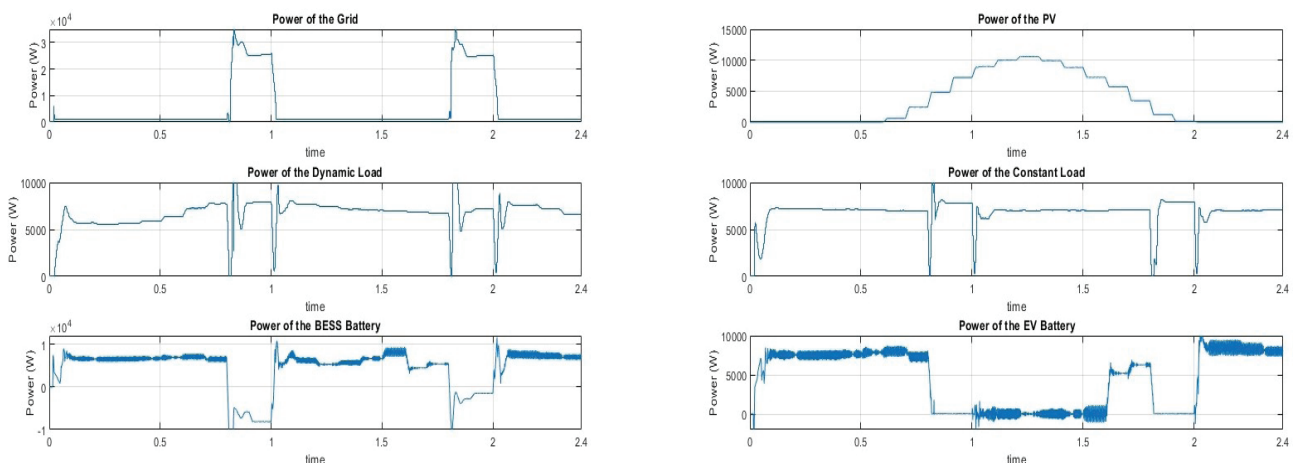


Figure 6. Shows the power results for OPF during normal condition.

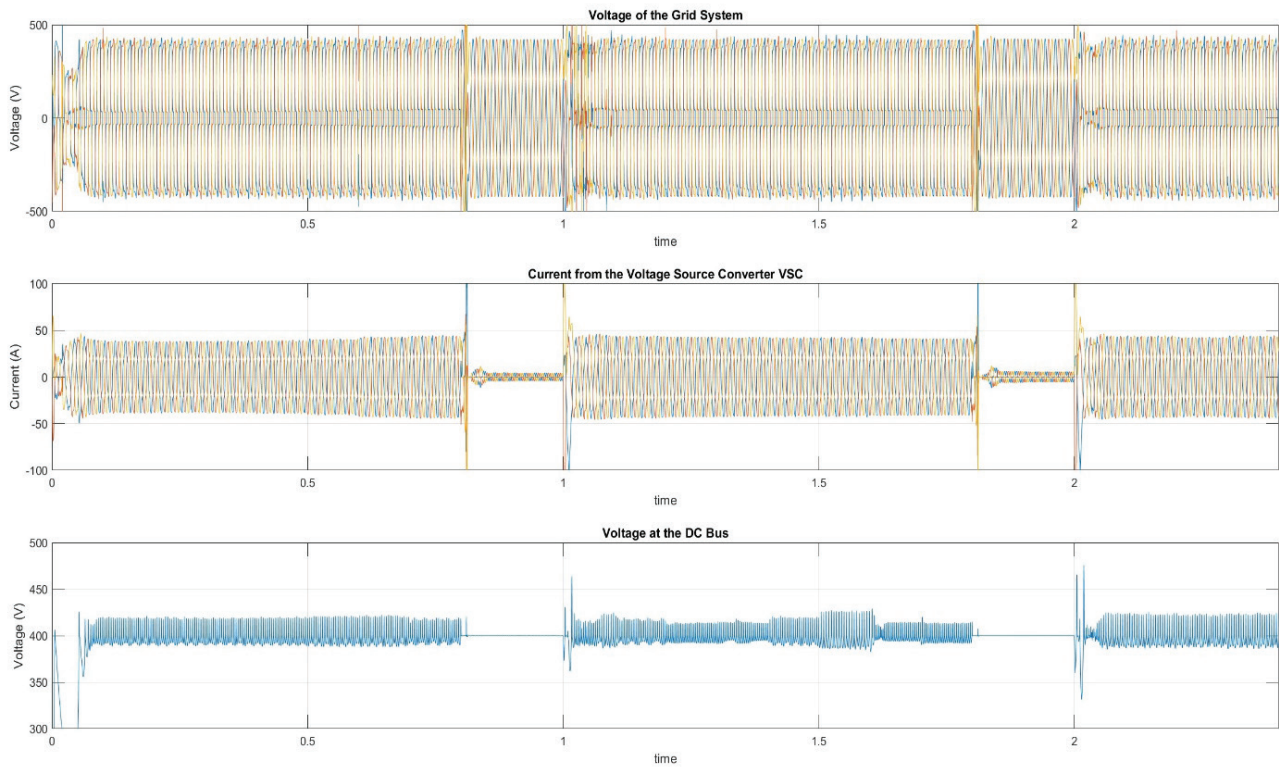


Figure 7. Voltage at the grid system, current at VSC, voltage at the DC bus for OPF in normal condition.

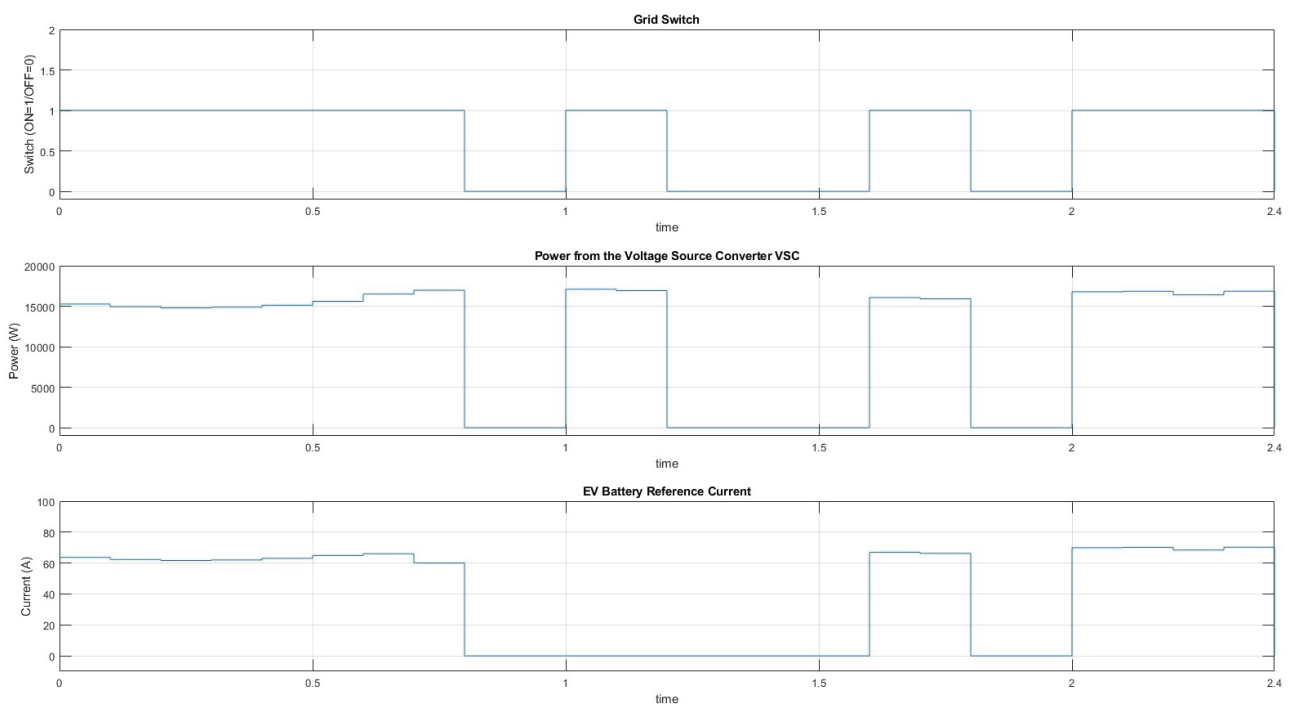


Figure 8. Shows the grid switch, power from the VSC, and the EV battery reference current in solar irradiance abnormal condition.

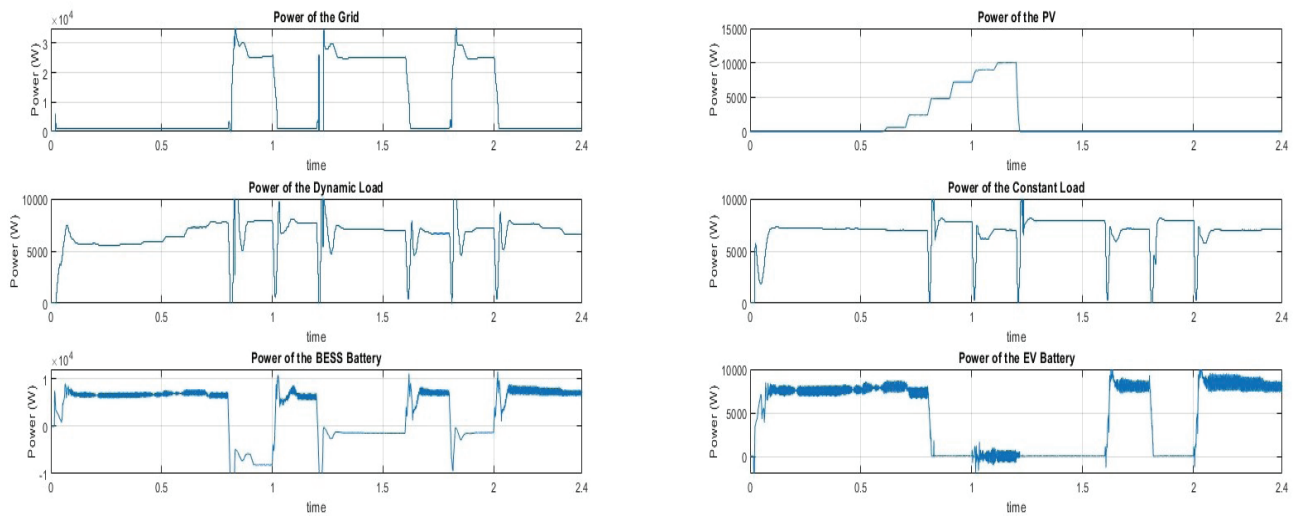


Figure 9. Shows the power results for OPF during solar irradiance abnormal condition.

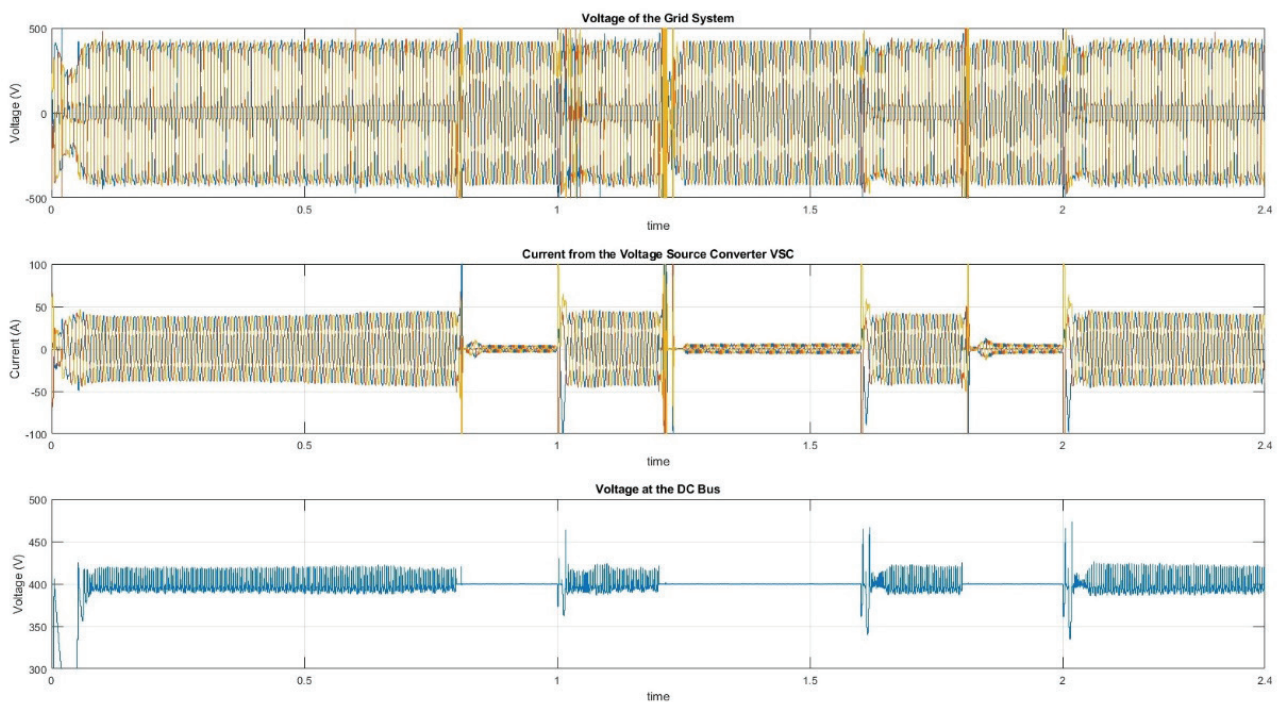


Figure 10. Voltage at the grid system, current at VSC, voltage at the DC bus for OPF in solar irradiance abnormal condition.

The results for voltage of the grid system, voltage at the DC bus, and current for the VSC are presented in Figure 10.

c. The State of Charge (SOC) for both the Battery Energy Storage System (BESS) and Electric Vehicle (EV) at 0% condition

The results for grid switch, power from the VSC, and the EV battery reference current are presented in Figure 11.

At state of zero charge for BESS and EV the MG system fully supported by the main grid power supply. The grid switch remains at grid-connected mode (switch=0).

The MG purpose is to balance power quality, overcome limitations, reduce power losses and enhance cost efficiency of a system. The OPF controller used as a power management strategy to effectively control the power flow of the system.

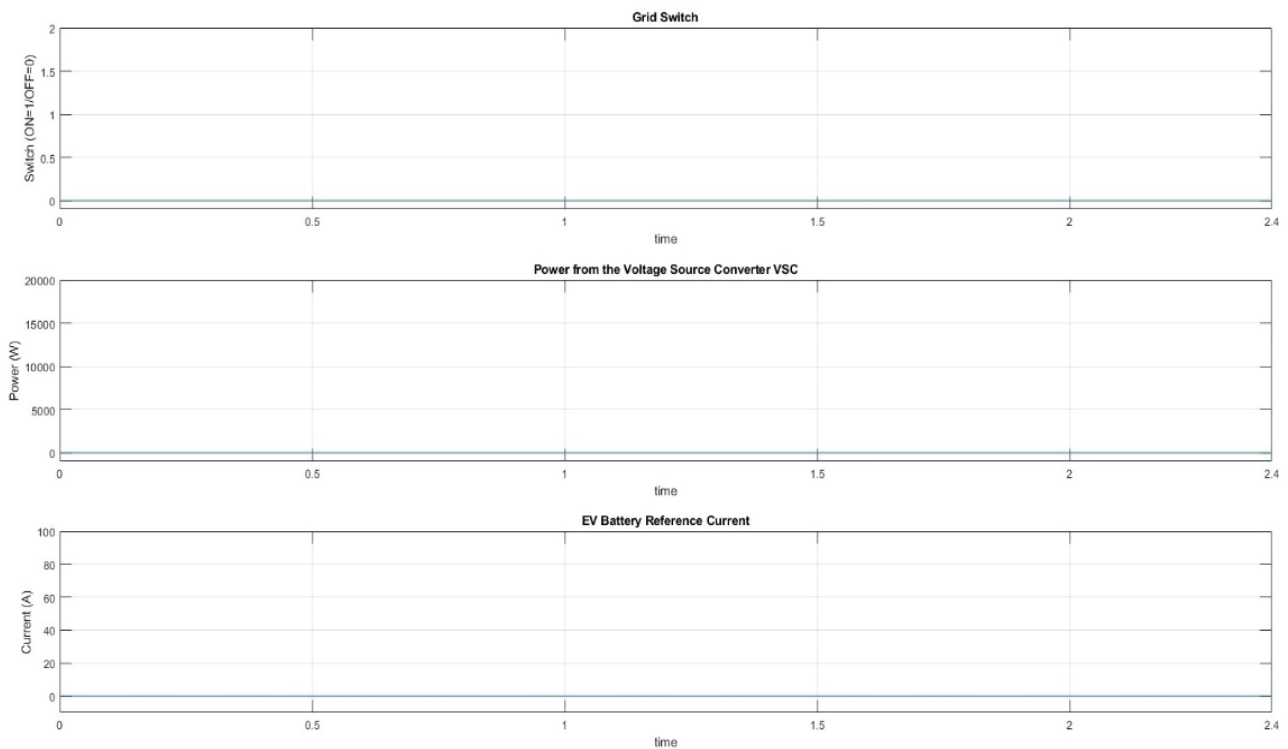


Figure 11. Shows the grid switch, power from the VSC, and the EV battery reference current in the EV, and BESS battery SOC 0% condition.

However, there are some ripples occurred when the switching modes changed from 0 to 1 or 1 to 0. These fluctuations need to be kept at minimum so the system can have much better performance both before and after switching modes. There are some works need to be done for future work. For future studies, the limitations such as fluctuations occurring immediately after switching modes, as observed in the results need to be reduced, and

the system can be analyzed in a microgrid system with a higher capacity to better understand the effect of the controller. Moreover, the number of power sources such as wind power, and other renewable energy sources can be added to the system. Hence, the proposed project can be realized in real project and the comparison between simulation and prototype will be verified and will be discussed further.

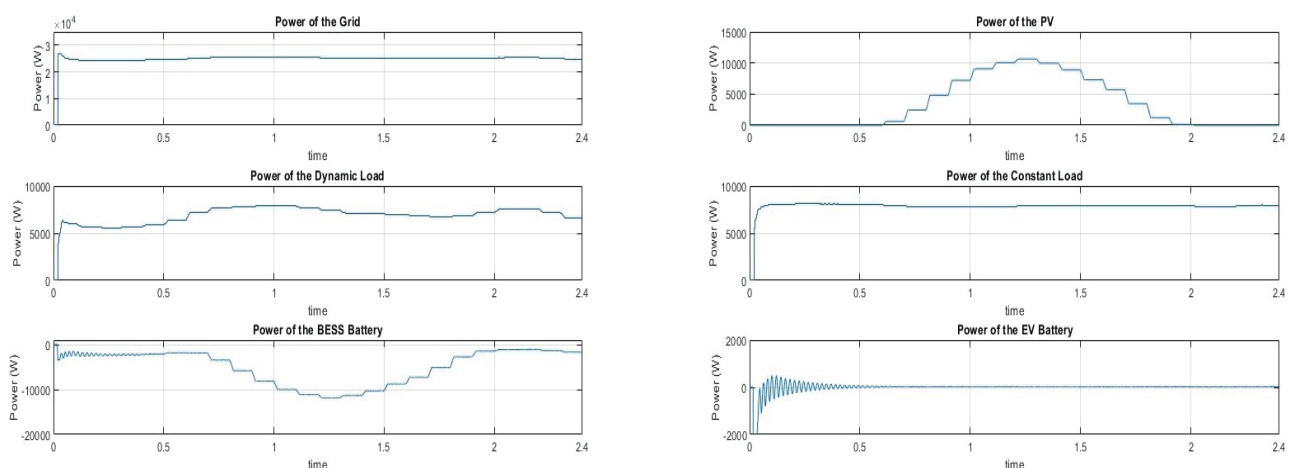


Figure 12. Shows the power results for OPF during EV and BESS battery SOC 0% condition.

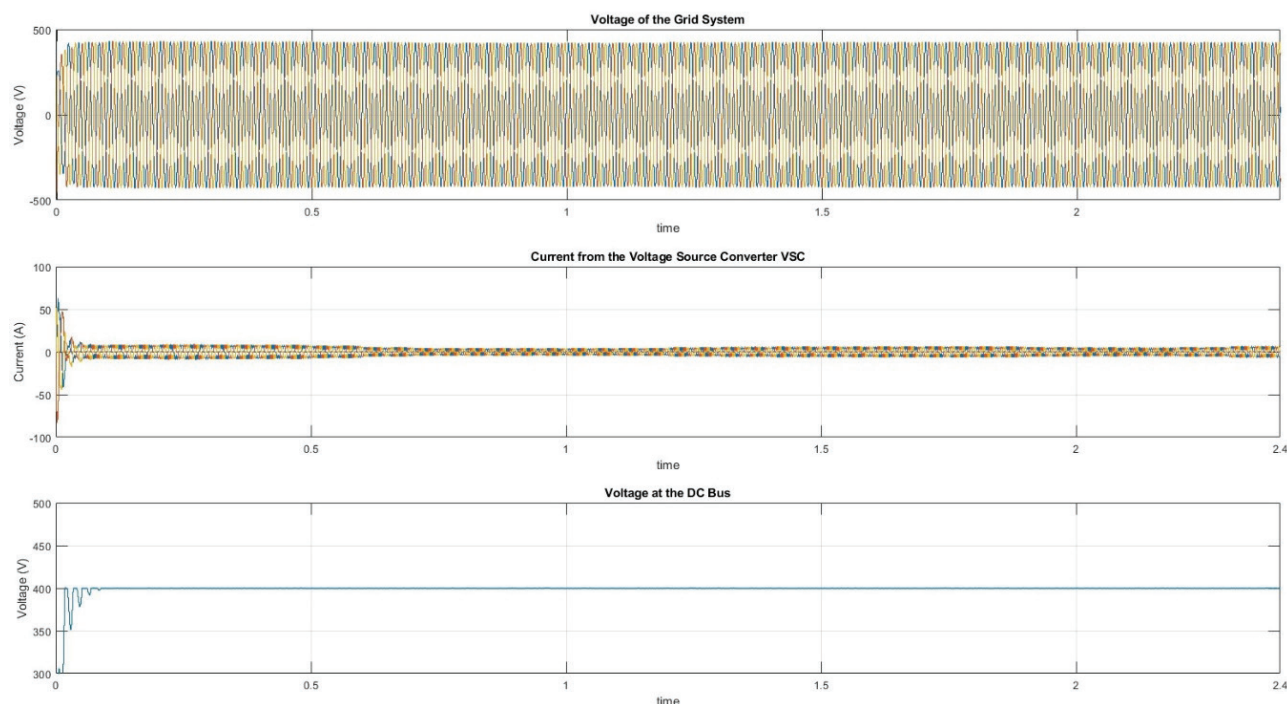


Figure 13. Voltage at the grid system, current at VSC, voltage at the DC bus for OPF in EV and BESS battery SOC 0% condition.

CONCLUSION

As the world rapidly advances, the use of renewable energy sources is also on the rise. To ensure efficient and reliable power distribution in Microgrid systems, power management strategies must be enhanced. The energy sources can experience disturbances, faults and fluctuations in parameters that's why the controllers are required to balance these disturbances. More research has been conducted to minimize instability in Microgrid system. Some researchers used PI controllers to improve the performance of the Microgrid system. However, this paper incorporated optimum power flow used as a centralized controller to control the switching mode between renewable energy source and main grid power. The Microgrid (MG) consists of dynamic load, constant load, solar PV, Battery Energy Storage system (BESS) and electrical vehicle battery, and a grid. The optimum power flow (OPF) is used to provide safe and economic operation of Power Systems. Some Real-life cases such as the uncertainty of load demand and the changing in Irradiance level which affect the microgrids efficiency have been taken into the account. The inputs of the OPF received information from Microgrid and processed them with an algorithm and presented output results for grid switch, reference power for voltage source converter and reference current for the EV battery. The results showed that the OPF can control the switching modes when the power supply from sources is lower than loads. After switching occurred there were ripples in the voltages, this is because of the

sudden change in grid switch. For future work it is necessary to improve the system for better performance and minimize the fluctuations in voltage at the grid and voltages at the DC bus.

The analysis and simulations indicate that the OPF based power management strategy can be implemented in a hybrid Microgrid system to enhance power flow, power supply efficiency and reliability of the system.

AUTHORSHIP CONTRIBUTIONS

Authors equally contributed to this work.

DATA AVAILABILITY STATEMENT

The authors confirm that the data that supports the findings of this study are available within the article. Raw data that support the finding of this study are available from the corresponding author, upon reasonable request.

CONFLICT OF INTEREST

The author declared no potential conflicts of interest with respect to the research, authorship, and/or publication of this article.

ETHICS

There are no ethical issues with the publication of this manuscript.

STATEMENT ON THE USE OF ARTIFICIAL INTELLIGENCE

Artificial intelligence was not used in the preparation of the article.

REFERENCES

- [1] Bragatto T, Carere F, Gatta FM, Geri A, Maccioni M, Simbolotti G. Electrical energy production from coal: Technical and economic performances during the last twenty years. In: 2022 IEEE International Conference on Environment and Electrical Engineering and 2022 IEEE Industrial and Commercial Power Systems Europe (EEEIC / I&CPS Europe). Prague, Czech Republic: IEEE; 2022. p. 1–6. [\[CrossRef\]](#)
- [2] Belge AT, Mishra S, Alegavi S. A review on alternative energy sources. In: 2022 5th International Conference on Advances in Science and Technology (ICAST). Mumbai, India: IEEE; 2022. p. 558–563. [\[CrossRef\]](#)
- [3] Lebsir A, Benamimour T. Renewable energies in the twenty-first century: A global-view. In: 2023 Second International Conference on Energy Transition and Security (ICETS). Adrar, Algeria: IEEE; 2023. p. 1–6. [\[CrossRef\]](#)
- [4] Wang Z, Jiang T, Liu G, Hu J, Lu S. Study on optimization of consumption and delivery scheme of high-proportion renewable energy grid in zero-carbon park based on cuckoo search. In: 2023 2nd International Conference on Clean Energy Storage and Power Engineering (CESPE). Xi'an, China: IEEE; 2023. p. 207–211. [\[CrossRef\]](#)
- [5] Swain A, Dash SS, Bastia S, Bagarty DP, Behera S. Source side control analysis of an AC microgrid fed with hybrid renewable distributed energy sources. In: 2020 3rd International Conference on Energy, Power and Environment: Towards Clean Energy Technologies. Shillong, India: IEEE; 2021. p. 1–5. [\[CrossRef\]](#)
- [6] Habibnia S, Mahdavi MS, Gharehpetian GB, Ahmadihangar R, Rosin A, Vinnikov D. A new master-slave based centralized control method for an AC microgrid with multiple distributed energy resources. In: 2022 IEEE 13th International Symposium on Power Electronics for Distributed Generation Systems (PEDG). Kiel, Germany: IEEE; 2022. p. 1–6. [\[CrossRef\]](#)
- [7] Pattnayak SK, Choudhury S, Nayak N, Bagarty DP, Biswabandhya M. Maximum power tracking & harmonic reduction on grid PV system using chaotic gravitational search algorithm based MPPT controller. In: 2020 International Conference on Computational Intelligence for Smart Power System and Sustainable Energy (CISPSSE). Keonjhar, India: IEEE; 2020. p. 1–6. [\[CrossRef\]](#)
- [8] Xiao W. Photovoltaic power system: Modelling, design and control. Hoboken, NJ: John Wiley & Sons; 2017. [\[CrossRef\]](#)
- [9] Baranzelli C, Lavallo C, Sgobbi A, Aurambot J, Trombetti J, Jacobs J, et al. Regional patterns of energy production and consumption factors in Europe: Exploratory project EREBILAND: European regional energy balance and innovation landscape. LU Regional patterns of energy production and consumption factors in Europe: Publications Office; 2016. Available at: <https://data.europa.eu/doi/10.2788/357099> Accessed on Nov 25, 2025.
- [10] Yilmaz A, Alkan A. Investigation of power system transient disturbances in frequency and time-frequency domains. SIGMA 2014;32:154–162.
- [11] Brandao DI, Ferreira WM, Alonso AMS, Tedeschi E, Marafao FP. Optimal multiobjective control of low-voltage AC microgrids: Power flow regulation and compensation of reactive power and unbalance. IEEE Trans Smart Grid 2020;11:1239–1252. [\[CrossRef\]](#)
- [12] Ekinci S. Power system stabilizer design for multi-machine power system using bat search algorithm. SIGMA 2015;33:627–633.
- [13] Pourbabak H, Alsafasfeh Q, Su W. A distributed consensus-based algorithm for optimal power flow in DC distribution grids. IEEE Trans Power Syst 2020;35:3506–3515. [\[CrossRef\]](#)
- [14] Hu J, Ma H. Distributed real-time optimal power flow strategy for DC microgrid under stochastic communication networks. J Mod Power Syst Clean Energy 2023;11:1585–1595. [\[CrossRef\]](#)
- [15] Eajal AA, Yazdavar AH, El-Saadany EF, Salama MMA. Optimizing the droop characteristics of AC/DC hybrid microgrids for precise power sharing. IEEE Syst J 2021;15:560–569. [\[CrossRef\]](#)
- [16] Mahouti P, Belen MA, Pa H, Güne F. Design of a high efficiency power amplifier for wireless and radar applications. 2015.
- [17] Kabak M, Taşkınöz G. Determination of the installation sites of wind power plants with spatial analysis. A model proposal. Sigma J Eng Nat Sci 2020;38:441–457.
- [18] Yasseen H, Csátár J. Power management strategy of AC/DC hybrid microgrids based on integrating battery SoC conditions to state logic control algorithm. In: 2024 12th International Conference on Smart Grid (icSmartGrid). Setubal, Portugal: IEEE; 2024. p. 727–731. [\[CrossRef\]](#)
- [19] Al-Ammar EA, Habib HUR, Waqar A, Wang S, Rahman MM, Ahmed A. Predictive direct power control of voltage source converters in microgrids during reconfiguration. In: 2020 Advances in Science and Engineering Technology International Conferences (ASET). Dubai, UAE: IEEE; 2020. p. 1–6. [\[CrossRef\]](#)
- [20] Singh S, Narayanan V, Singh B, Panigrahi BK. Multiple voltage source converters based microgrid

- with solar photovoltaic array and battery storage. *e-Prime Adv Electr Eng Electron Energy* 2024;7:100408. [\[CrossRef\]](#)
- [21] Ganesan S, Nagarajan AP. An efficient buck-boost converter for fast active balancing of lithium-ion battery packs in electric vehicle applications. *Comput Electr Eng* 2024;118:109429. [\[CrossRef\]](#)
- [22] Abdel-Moneim MG, Hamad MS, Abdel-Khalik AS, Hamdy RR, Hamdan E, Ahmed S. Analysis and control of split-source current-type inverter for grid-connected applications. *Alex Eng J* 2024;96:268–278. [\[CrossRef\]](#)
- [23] Shayeghi H, Rahn timer A, Takorabet N, Thounthong P, Bizon N. Designing a multi-stage PD(1+PI) controller for DC–DC buck converter. *Energy Rep* 2022;8:765–773. [\[CrossRef\]](#)
- [24] Rousis AO, Konstantelos I, Strbac G. A planning model for a hybrid AC–DC microgrid using a novel GA/AC OPF algorithm. *IEEE Trans Power Syst* 2020;35:227–237. [\[CrossRef\]](#)
- [25] Khan MN, Schulz NN. An optimal neighborhood energy sharing scheme applied to islanded DC microgrids for cooperative rural electrification. *IEEE Access* 2023;11:116956–116966. [\[CrossRef\]](#)
- [26] Derbas AA, Kheradmandi M, Hamzeh M, Hatzargyriou ND. A hybrid power sharing control to enhance the small signal stability in DC microgrids. *IEEE Trans Smart Grid* 2022;13:1826–1837. [\[CrossRef\]](#)
- [27] Ghosh SS, Chattopadhyay S, Das A, Medikundu NR, Almawgani AHM, Alhawari ARH, et al. Wavelet-based rapid identification of IGBT switch breakdown in voltage source converter. *Microelectron Reliab* 2024;152:115283. [\[CrossRef\]](#)
- [28] Liu J, Liu J, Zhao Y. A unified control strategy for three-phase inverter in distributed generation. *IEEE Trans Power Electron* 2014;29:1176–1191. [\[CrossRef\]](#)
- [29] Kumar N, Saha TK, Dey J. Multilevel inverter (MLI)-based stand-alone photovoltaic system: Modeling, analysis, and control. *IEEE Syst J* 2020;14:909–915. [\[CrossRef\]](#)
- [30] Soheli SN, Sarowar G, Hoque MA, Hasan MS. Design and analysis of a DC–DC buck boost converter to achieve high efficiency and low voltage gain by using buck boost topology into buck topology. In: 2018 International Conference on Advancement in Electrical and Electronic Engineering (ICAEEE). Gazipur, Bangladesh: IEEE; 2018. p. 1–4. [\[CrossRef\]](#)
- [31] Wu F, Fan S, Li X, Luo S. Bidirectional buck–boost current-fed isolated DC–DC converter and its modulation. *IEEE Trans Power Electron* 2020;35:5506–5516. [\[CrossRef\]](#)
- [32] Eajal AA, El-Saadany EF, Ponnambalam K. Optimal power flow for converter-dominated AC/DC hybrid microgrids. In: 2017 IEEE International Conference on Industrial Technology (ICIT). Toronto, Canada: IEEE; 2017. p. 603–608. [\[CrossRef\]](#)
- [33] Aljribi SFA. Optimal power flow for hybrid AC–DC microgrid. International Renewable and Sustainable Energy Conference (IRSEC), 2022.
- [34] Ravada BR, Tummuru NR. Control of a supercapacitor-battery-PV based stand-alone DC-microgrid. *IEEE Trans Energy Convers* 2020;35:1268–1277. [\[CrossRef\]](#)
- [35] Chellakhi A, El Beid S, Abouelmahjoub Y, Mchaouar Y. An efficient implementation of three-level boost converter with capacitor voltage balancing for an advanced MPPT approach in PV systems. *e-Prime Adv Electr Eng Electron Energy* 2024;9:100688. [\[CrossRef\]](#)
- [36] Zhong QC, Ming WL, Zeng Y. Self-synchronized universal droop controller. *IEEE Access* 2016;4:7145–7153. [\[CrossRef\]](#)
- [37] Wang Y, Liu Y, Bian J, Ji R. DC voltage control strategy research in multi-terminal HVDC system based on optimal AC/DC power flow. In: 2016 IEEE PES Asia-Pacific Power and Energy Engineering Conference (APPEEC). Xi'an, China: IEEE; 2016. p. 1948–1952. [\[CrossRef\]](#)
- [38] Hamidieh M, Ghassemi M. Microgrids and resilience: A review. *IEEE Access* 2022;10:106059–106080. [\[CrossRef\]](#)
- [39] Pathan J. Model predictive control of DC–DC buck converter and its comparison with PID controller.
- [40] Nabatirad M, Razzaghi R, Bahrani B. Decentralized energy management and voltage regulation in islanded DC microgrids. *IEEE Syst J* 2022;16:5835–5844. [\[CrossRef\]](#)
- [41] Ortmeyer T, Daryanian B, Datka P, Freeman L, Burns C. Design and benefit cost analysis of the Potsdam microgrid. In: 2022 IEEE Power & Energy Society General Meeting (PESGM). Denver, USA: IEEE; 2022. p. 1–5. [\[CrossRef\]](#)
- [42] Liu T, Lai Y, Xue A, Yin Y, Chen Y, Yin X. Research and application of AC&DC hybrid power grid stability control technology. In: 2023 8th Asia Conference on Power and Electrical Engineering (ACPEE). Tianjin, China: IEEE; 2023. p. 2445–2449. [\[CrossRef\]](#)
- [43] Peng S, Xie N, Wang C. A self-adaptive power flow analysis methodology for AC/DC hybrid system. *IEEE Trans Power Deliv* 2023;38:2261–2273. [\[CrossRef\]](#)
- [44] Fleischhacker A, Corinaldesi C, Lettner G, Auer H, Botterud A. Stabilizing energy communities through energy pricing or PV expansion. *IEEE Trans Smart Grid* 2022;13:728–737. [\[CrossRef\]](#)
- [45] Saif A, Khadem SK, Conlon MF, Norton B. Impact of distributed energy resources in smart homes and community-based electricity market. *IEEE Trans Ind Appl* 2023;59:59–69. [\[CrossRef\]](#)
- [46] Shehzad M, Jamal N, Muqet HA, Mirsaeidi S, Muttaqi KM. Cost effective analysis of stationary and mobile energy storage systems in prosumer

microgrid considering system reliability and real-time pricing scheme. In: 2023 IEEE International Conference on Energy Technologies for Future Grids (ETFG). Wollongong, Australia: IEEE; 2023. p. 1–5. [CrossRef]

- [47] Statnett. Rep data from the power system industry, 2021. Available at: <https://www.statnett.no/en/for-stakeholders-in-the-power-industry/>

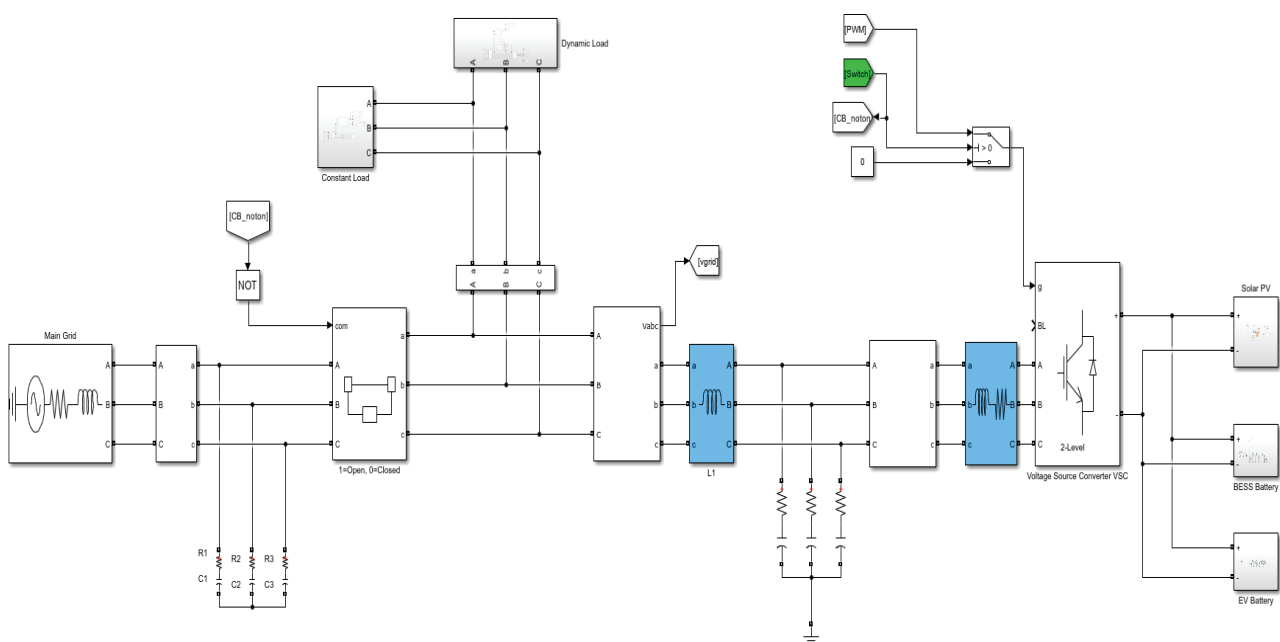
data-from-the-power-system/ Accessed on Feb 07, 2024.

- [48] EU Science Hub. European Commission, Photovoltaic Geographical Information System (PVGIS) data 2023. Available at: https://joint-research-centre.ec.europa.eu/photovoltaic-geographical-information-system-pvgis_en Accessed on Feb 07, 2024.

APPENDICES

APPENDIX 1

The hybrid MG system with necessary components are given in Appendix 1.



Appendix 1. Shows the complete model of the hybrid MG system used in this paper.